

# Paced Electrogram Fractionation Analysis of Arrhythmogenic Tendency in $\Delta$ KPQ *Scn5a* Mice

CATHERINE E. HEAD, M.B., B.CHIR., F.R.C.P., PH.D.,\* RICHARD BALASUBRAMANIAM, M.B., CH.B., M.R.C.P.,\* GLYN THOMAS, M.B.B.S., M.R.C.P.,† CATHARINE A. GODDARD, PH.D.,‡ MING LEI, M.D., D.PHIL.,‡ WILLIAM H. COLLEDGE, PH.D.,\* ANDREW A. GRACE, F.R.C.P., PH.D.,‡ and CHRISTOPHER L-H. HUANG, B.M., B.Ch., D.M., Sc.D.\*

From the \*Physiological Laboratory, University of Cambridge, Downing Street, Cambridge; †Section of Cardiovascular Biology, Department of Biochemistry, University of Cambridge, Tennis Court Road, Cambridge; and ‡Laboratory of Physiology, University of Oxford, Oxford, UK

**Arrhythmogenesis in  $\Delta$ KPQ *Scn5a* (Long QT 3) Mice.** *Introduction:* Gain-of-function mutations within *Scn5a*, including the  $\Delta$ KPQ 1505-1507 deletion in the inactivation domain compromising myocardial repolarization, are implicated in human long QT 3 syndrome (LQT3), associated with ventricular arrhythmogenesis and sudden death.

*Methods and Results:* Patch clamp studies on isolated ventricular *Scn5a*+/ $\Delta$  myocytes from  $\Delta$ KPQ mice produced by homologous recombination in embryonic stem (ES) cells confirmed such altered electrophysiological properties of the mutant channel. Programmed electrical stimulation (PES) with decremental pacing from the basal right ventricular epicardial surface and paced electrogram fractionation analysis (PEFA) of electrograms recorded from the basal left ventricular epicardial surface of Langendorff-perfused whole heart preparations demonstrated ventricular tachycardia (VT) in 8 of 9 *Scn5a*+/ $\Delta$  mutant (but no *Scn5a*+/+ (wild-type (WT)) controls; n = 17), with increased electrogram durations (EGD) and more dispersed conduction curves. Isoproterenol (100 nM) was without effect on tachycardic *Scn5a*+/ $\Delta$  hearts (n = 9) yet propranolol (1  $\mu$ M) prevented VT in all isoproterenol-infused WT control (n = 4) but no *Scn5a*+/ $\Delta$  hearts (n = 4). Furthermore propranolol itself increased EGD and dispersion in *Scn5a*+/ $\Delta$  hearts. In contrast, mexiletine (10  $\mu$ M) suppressed VTs in 4 of 5 *Scn5a*+/ $\Delta$  hearts without altering EGD or dispersion.

*Conclusion:*  $\beta$ -adrenoreceptor blockade does not confer an antiarrhythmic effect and may even enhance arrhythmogenesis by increasing reentrant substrate in *Scn5a*+/ $\Delta$  hearts while mexiletine protects against VT without modifying conduction characteristics. Together these findings permit a scheme where VT in LQT3 is initiated by triggered mechanisms but propagated by reentry. (*J Cardiovasc Electrophysiol*, Vol. 16, pp. 1-12, November 2005)

*long QT 3 syndrome (LQT3), ventricular arrhythmogenesis, sudden death, paced electrogram fractionation analysis, Scn5a gain-of-function mutations*

## Introduction

Human long QT syndromes (LQTS), associated with potentially fatal ventricular arrhythmias, reflect inherited abnormalities in cardiac excitability that delay myocardial repolarization. Increased ventricular action potential durations (APD) characteristically prolong the electrocardiographic

QT interval. Most LQTS cases reflect loss-of-function mutations in K<sup>+</sup> channel genes but at least seven ion channel subunit genes are implicated in LQTS.<sup>1-3</sup> Voltage-gated Na<sup>+</sup> channels generate the rapid inward currents causing the initial depolarization in cardiac action potentials (APs); mutations in the *Scn5a* gene encoding their  $\alpha$ -(pore-forming) subunit have been implicated in the Brugada and Lenegre arrhythmic syndromes as well as in LQTS.<sup>3-7</sup> *Scn5a* mutations can increase late Na<sup>+</sup> currents, prolong action potential plateaus, and delay repolarization, predisposing to early afterdepolarizations (EADs) resulting from L-type Ca<sup>2+</sup> channel activation<sup>8</sup> that can trigger torsade de pointes (TdP).<sup>9</sup> Varying ion channel expression patterns between endocardial, epicardial and midmyocardial (M) cells cause electrical heterogeneity through the ventricular wall and a transmural dispersion of repolarization.<sup>10</sup> This is accentuated by increased late Na<sup>+</sup> currents, I<sub>Na</sub>, which preferentially prolong M cell APDs over those of the epicardium or endocardium thus generating reentrant substrate that maintains the arrhythmia.<sup>11</sup>

Clinical LQT3 shows a number of important contrasts from the other LQTS variants: (1)  $\beta$ -agonists reduce APD and protect against TdP<sup>12</sup> paralleling clinical findings that most LQT3 events occur during sleep whereas cardiac events

This study was supported by grants from the British Heart Foundation, the Medical Research Council, the Wellcome Trust, the Leverhulme Trust, the Helen Kirkland Fund for Cardiac Research, and the Raymond and Beverly Sacker Medical Research Centre.

C.E. Head, R. Balasubramaniam, and G. Thomas were equal contributors to this article.

Address for correspondence: C. L-H. Huang, B.M., B.Ch., D.M., Sc.D., Physiological Laboratory, University of Cambridge, Downing Street, Cambridge CB2 3EG, United Kingdom. Fax: 044-1223-333840; E-mail: chl11@cam.ac.uk

Manuscript received 10 February 2005; Revised manuscript received 25 March 2005; Accepted for publication 1 April 2005.

doi: 10.1111/j.1540-8167.2005.50086.x

in LQT1 and LQT2 mainly occur during exercise or states of arousal.<sup>13</sup> (2) Carriers of the  $\Delta$ KPQ LQT3 mutation show slowed atrial, atrioventricular, and ventricular conduction, though most were on  $\beta$ -blockers when examined.<sup>14</sup> (3) Death in at least some LQT3 mutation carriers is associated with bradycardic rather than tachycardic changes.<sup>15</sup>

The present experiments adapt a pacing and analysis technique used to stratify arrhythmic risk in LQTS patients<sup>16,17</sup> to investigate whether mouse hearts that offer a genetically manipulable experimental system, might model and quantify these features of LQT3 for translation into studies of potential arrhythmogenic human phenotypes. We introduced a  $\Delta$ KPQ 1505–1507 deletion in the channel inactivation domain into the mouse genome by homologous recombination in embryonic stem (ES) cells, then compared (1) AP waveforms from isolated ventricular myocytes from wild-type (WT) and *Scn5a*+/ $\Delta$  hearts by whole-cell patch clamping, (2) electrophysiological phenotypes of whole ex vivo isolated Langendorff-perfused WT and *Scn5a*+/ $\Delta$  hearts, and (3) investigated effects of  $\beta$ -adrenergic agonists and antagonists and Na<sup>+</sup> channel blockade on arrhythmogenic properties of *Scn5a*+/ $\Delta$  hearts to explore parallels with human LQT3. A gene-targeted mouse model of LQT3 has been created simultaneously elsewhere by the introduction of the  $\Delta$ KPQ mutation into *Scn5a*<sup>18</sup> using a similar targeting strategy; phenotypes of these two lines are discussed and compared.

## Materials and Methods

### Generation of Mice Heterozygous for the $\Delta$ KPQ Mutation (*Scn5a* +/ $\Delta$ )

Primers corresponding to known rat *Scn5a* exon 23 and 27 sequences were used to amplify a 6 kb fragment from WT 129SvEv mouse genomic DNA. A 9 bp deletion ( $\Delta$ KPQ) and associated restriction sites (HindIII and BamHI) were introduced into exon 26 by a polymerase chain reaction (PCR) megaprimer technique. A 1.6 kb piece was amplified using a 5' primer carrying the desired mutation in exon 26 and a 3' primer in exon 27. A second round PCR used this 1.6 kb mutant fragment to anneal to the WT 6 kb exon 23–27 fragment. A 6 kb fragment (pG32) carrying the desired mutation was cloned from the PCR products using the pGEM-T vector (Stratagene). All exons and intron/exon junctions were sequenced. pKO3'/DT-A (new) was a gift from Dr. M Snaith (Dept. of Genetics, Cambridge University, UK). The *PGKDTA* cassette was cloned into a *Sac*II site at the 3' end of the vector as negative selection against random integration.<sup>19</sup> A selectable marker *thymidine kinase/neomycin*, flanked by *loxP* sites, was cloned in to the *Nhe*I site in intron 26 of the *Scn5a* piece. The vector was linearized at a unique *Not*I site at the 5' end of homology and electroporated into 129SvEv embryonic stem cells. Successful targeting to the *Scn5a* locus was identified by PCR with primers Mint25F (GGACCCTGGAAAGGCAGATTTGG), Mint27R (CCGTCCAGCCAACTTGCATACC), and PGKP2 (ATGCTCCAGACTGCCTTGGGAAA), in only one (clone 179) out of 132 samples screened. Correct targeting was confirmed by Southern transfer analysis at both ends using a *Bgl*III digest and external probes (Fig. 1), and additionally at the 5' end using an *Nco*I digest. After confirmation of correct chromosome number and targeting using fluorescent in situ hybridization (FISH), the selection cassette was removed from

one population of targeted ES cells by electroporation of a Cre recombinase expressing plasmid. Successful removal was selected by growth in ganciclovir-containing medium and screened by PCR: primers Hex26F (GGCCAGGACATCTTCATGACAG) and Mscnint26R2 (CCATGACC-AACTCTTCATCCC) amplified a band 150 bp larger in the Cre-*lox* than in the WT allele, a difference corresponding to the remaining *loxP* site and associated vector sequence not removed by the Cre recombination. All clones screened appeared to have undergone successful removal of their selection cassette. This was confirmed by Southern blot of a *Bgl*III digest with firstly a 3' probe, the removal of the selection cassette containing the additional *Bgl*III site leaving only the WT band, and secondly a *neo* probe, no band present once the selection cassette was removed.

ES cells with and without the selection cassette were used for injection into C57BL/6J blastocysts as previously described,<sup>20</sup> generating male chimaeras subsequently mated with C57BL/6J females. Germline transmission was defined by the presence of agouti offspring. Consistent with the findings of other groups,<sup>21,22</sup> the retention of the HSV-1 *TK* gene conferred male sterility if expressed in the germ line. Hence the only offspring from a 179 chimaera with the selection cassette were derived from the host blastocyst. Germ line chimaeras were subsequently bred with 129 Sv/Olac mice to generate an inbred line. Agouti offspring were genotyped using a variant of the PCR used to screen for the removal of the *neo/TK* cassette. Mint25F2 (GCGGGTGCTGTCTTC-TACTTAGG) was used in place of Hex26F because the latter also hybridizes to *Scn10a*.

### Examination and Genotyping of Heterozygote Mating Embryos

Pregnant females were killed by a schedule 1 method 9.5–10.5 days postcoitum and the uterus removed to sterile phosphate buffered saline (PBS) on ice. Embryos were dissected free of the deciduum and extraembryonic membranes, the yolk sac stored at –20°C for genotyping, and the embryo photographed and either put into 10% neutral buffered formalin for paraffin blocking or flash frozen in liquid nitrogen for later RNA preparation and RT-PCR. Sagittal 6–10  $\mu$ m sections were cut from the paraffin blocks and stained with hematoxylin and eosin (Histopathology Laboratory, Department of Clinical Veterinary Medicine, University of Cambridge, Cambridge, UK).

### Experimental Animals

Mice were maintained at room temperature and 12 hour light/dark cycles, fed with sterile rodent chow with free access to water. Experiments used mice aged 3–6 months. Offspring from heterozygote breeding pairs was genotyped, weaned, and used when of correct age. Mice were bred and used in accordance with the U.K. Home Office Animals (Scientific Procedures) Act 1986.

### Patch Clamp Electrophysiology

Current and voltage clamping used an Axopatch-200B patch clamp amplifier. Electrical signals were simultaneously displayed and digitized by a DigiData 1200 AD converter for disk storage for later analysis using PCLAMP8 software (Axon Instruments Inc., Foster City, CA, USA). Capacitance current transients were electronically subtracted with

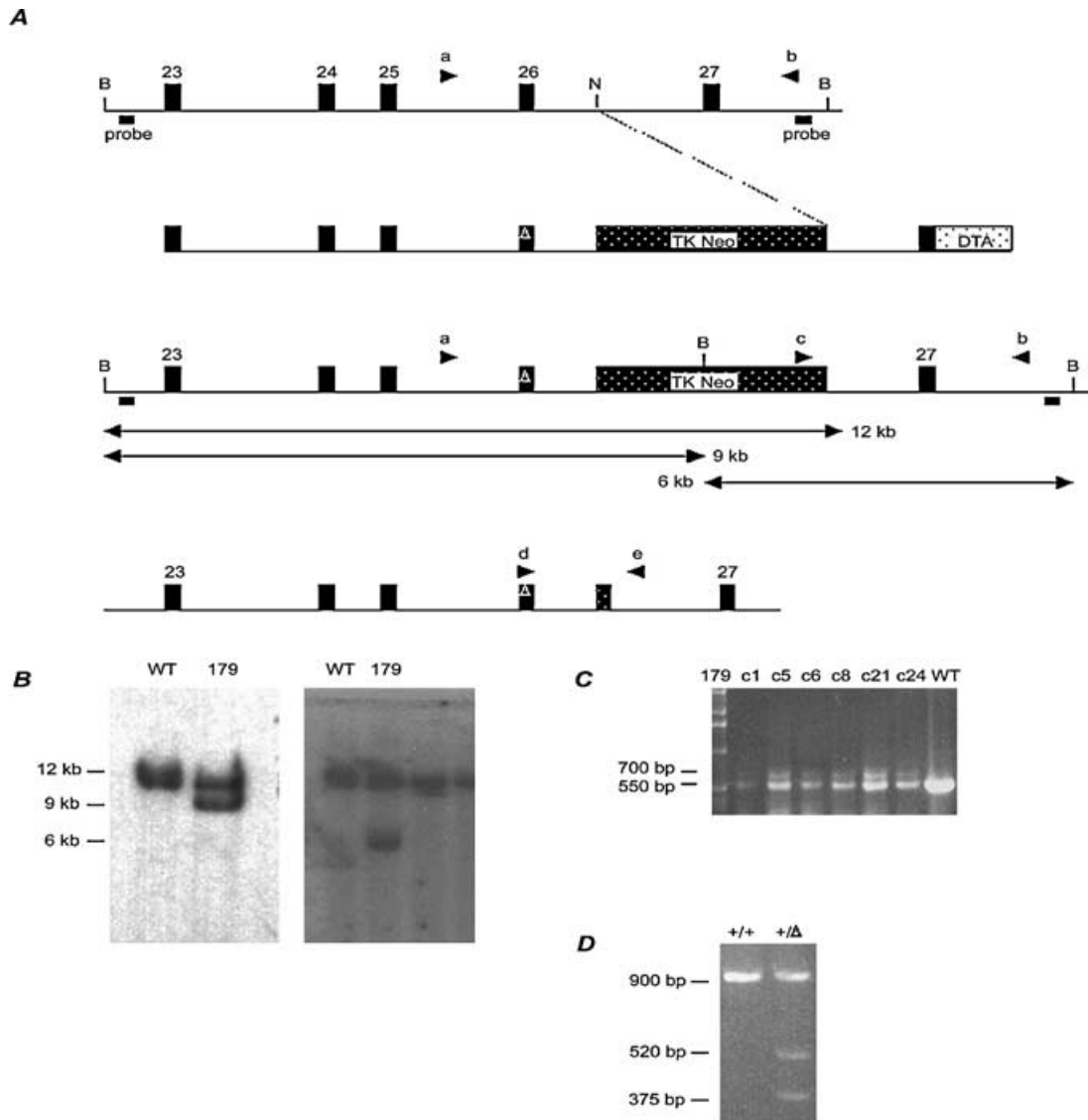


**Figure 1.** Targeting strategy for the generation of  $\Delta$ KPQ heterozygous ES cells. **A:** Schematic maps of the wild-type (WT) locus, the targeting construct, and the targeted locus before and after transient Cre expression in the embryonic stem cells. N = Nhe I; B = Bgl II; TK = thymidine kinase; DTA = diphtheria toxin gene. The TK/Neo cassette is flanked by loxP sites.  $\Delta$  denotes the 9 bp KPQ deletion. Successful targeting to the *Scn5a* locus was identified by PCR with primers a – Mint25F, b – Mint27R, and c – PGKP2, and confirmed by Southern transfer analysis at both ends using the external probes indicated: 5' probe, 330 bp EcoR I/Nde I fragment of intron 22; 3' probe, 700 bp Nde I/Xho I fragment of intron 27. Expected fragment sizes of WT and mutant alleles after digestion with Bgl II are shown. Removal of the TK/Neo cassette by electroporation of a Cre-expressing plasmid was selected by growth on ganciclovir-containing medium and confirmed by PCR with primers d – Hex26F and e – Mscnint26R2. A single loxP site and associated sequence (150 bp) remained, indicated by the small dotted rectangle. **B:** Southern blot of Bgl-II-digested ES cell DNA probed with 5' probe on the left and 3' probe on the right, showing the correctly targeted clone 179. **C:** PCR screen of ES cell clones surviving growth on ganciclovir-containing medium, using primers d and e with WT control. All survivors show the expected WT band size (550 bp) and in addition the 700 bp band indicating the presence of the remaining loxP site. **D:** Expression of the mutant allele. Reverse transcription-PCR with primers KPQF (CGTGAACAACAAGAGCGAGTG) and KPQR (TGCCGAAGATGGAGTAGATGA) generated a product of 896 bp from the  $\Delta$ KPQ allele (905 bp from the WT allele), digested into fragments of 521 bp and 375 bp by Bam HI at the introduced silent restriction site.

~80% series resistance compensation. Current signals were filtered at 10 kHz and sampled at 20 kHz. All current traces were leak-subtracted offline. Enzymatically dissociated adult ventricular myocytes were prepared from WT and *Scn5a* $\Delta$ /+ mice.<sup>23</sup> After cervical dislocation, the aorta was cannulated in situ, and the heart excised and perfused with oxygenated, warmed, nominally Ca<sup>2+</sup>-free Tyrode solution (mM: NaCl 130, KCl 5.4, MgCl<sub>2</sub> 3.5, NaH<sub>2</sub>PO<sub>4</sub> 0.4, HEPES 5, taurine 20, and glucose 10), followed by a solution containing 240 U/mL collagenase II (Worthington Biomedical Co., NJ,

USA), 0.075 mg/mL protease (Sigma-Aldrich, Poole, UK), and 50  $\mu$ M CaCl<sub>2</sub>. The LV free wall was isolated and gently agitated at 37°C in a collagenase solution containing 50  $\mu$ M CaCl<sub>2</sub>. Dispersed cells were washed twice in BSA then resuspended in a storage solution of DMEM supplemented with 2 mg/mL Ultraser G (Gibco BRL, Paisley, UK). Cells were stored at room temperature and used within 6–8 hours of isolation.

Membrane potentials were recorded at 37  $\pm$  0.5°C and membrane currents at room temperature ( $\approx$ 22°C) using

TABLE 1

Distribution of Genotypes of 3–4-Week-Old Mice (Expected Mendelian Frequencies in Brackets)

Mouse	+/+ (n)	+/ $\Delta$ (n)	Significance
Outbred	181 (154.3)	282 (308.6)	P < 0.01
Inbred	129 (99.7)	170 (199.3)	P < 0.005

patch pipettes (0.8–2.0 M  $\Omega$ ) pulled from 1.5 mm borosilicate glass containing internal filament (Clark Electromedical Instruments, Pangbourne, UK): (1) APs were recorded in current-clamped myocytes held at  $-80$  mV (stimulation frequency, 1 Hz) in Tyrode solution (mM: NaCl 140, KCl 4, CaCl<sub>2</sub> 2, MgCl<sub>2</sub> 2, HEPES 5, and glucose 5; pH 7.4) using pipettes filled with (mM) KCl 140, NaCl 10, EGTA 2, MgCl<sub>2</sub> 1, MgATP 5, and HEPES 10; pH 7.3). (2)  $I_{Na}$  was recorded in voltage-clamped myocytes superfused with modified Tyrode's solution (mM: NaCl 10, MgCl<sub>2</sub> 1.0, CaCl<sub>2</sub> 0.1, glucose 10, CsCl 130, and Hepes 10; pH 7.4) containing nifedipine (10  $\mu$ M) to block  $I_{Ca}$  using pipettes filled with (mM): NaCl 2, CsCl 140, HEPES 10, and EGTA 10; pH 7.4. (3) Experiments investigating activation characteristics imposed 10 msec pulses repeated at 10 Hz to test potentials between  $-120$  and  $+40$  mV on myocytes held at  $-120$  mV. (4) Investigations of steady state  $Na^+$  current inactivation subjected fibers initially held at  $-120$  mV to a double pulse protocol repeated at 2 Hz consisting of a 100 msec prepulse to test potentials between  $-120$  and 20 mV followed by a standard 10 msec test pulse to  $-30$  mV. (5) Experiments examining recovery from inactivation applied a triple pulse procedure repeated in 2 Hz cycles to myocytes initially held at  $-120$  mV. An initial 50 msec pulse to a membrane potential of  $-30$  mV was followed by pulses to a  $-120$  mV recovery level for 0.5, 1, 1.5, 2, 2.5, 3, 4, 5, 7, 7.5, 10, 15, 20, 25, 30, 40, 50 msec, respectively. A final 10 msec pulse to a membrane potential of  $-30$  mV then assessed extent of recovery. (6) Late  $Na^+$  currents were measured in myocytes held at  $-120$  mV in the presence of 135 mM external and 10 mM internal NaCl and CsCl, nifedipine (10  $\mu$ M) and ouabain (10  $\mu$ M) to block  $K^+$ ,  $Ca^{2+}$  and Na-Ca exchange current, respectively: test pulses of duration 100 msec to a membrane potential of  $+40$  mV were repeated at cycle frequencies of 2 Hz. (7) AP clamp experi-

ments<sup>24</sup> applied ten APs prerecorded ( $37 \pm 0.5^\circ\text{C}$ ) following formation of stable whole-cell current clamp configurations to the same cell in voltage clamp mode.

### Electrophysiological Studies in Langendorff-Perfused Preparations<sup>25–27</sup>

Whole hearts from mice given 100 i.u. intraperitoneal heparin 10 minutes before killing by cervical dislocation (Schedule 1: UK Animals [Scientific Procedures] Act 1986) were excised and placed in ice-cold bicarbonate-buffered Krebs-Henseleit solution (mM: NaCl 119, NaHCO<sub>3</sub> 25, KCl 4, KH<sub>2</sub>PO<sub>4</sub> 1.2, MgCl<sub>2</sub> 1, CaCl<sub>2</sub> 1.8, glucose 10, and Na-pyruvate 2, pH 7.4) bubbled with 95% O<sub>2</sub>/5% CO<sub>2</sub>. A small (3–4 mm) section of aorta was cannulated under the buffer surface and sutured to a 21-gauge tailor-made cannula, prefilled with ice-cold buffer solution, then used for retrograde perfusion using the above solution at 2–2.5 mL min<sup>-1</sup> using a peristaltic pump (Watson-Marlow Bredel model 505S, Falmouth, Cornwall, UK) after passing through 200  $\mu$ m and 5  $\mu$ m filters (Millipore, Watford, UK) and warming to 37°C via a water jacket and circulator (Techne model C-85A, Cambridge, UK). Healthy, viable hearts suitable for experimentation regained a healthy pink coloration and spontaneous rhythmic contraction with warming.

Programmed electrical stimulation (PES) of the heart (cf<sup>16,17</sup>) placed paired (1-mm interpole spacing) platinum stimulating and recording electrodes on the basal epicardial surfaces of the right and left ventricles, respectively. Initial pacing used 2 msec square-wave stimuli with amplitudes three times excitation threshold (Grass S48 stimulator, Grass-Telefactor, Slough, UK) for 20 minutes at 10 Hz. Subsequent PES procedures first applied standard pacing stimuli (8 or 10 Hz) for 20 seconds. Drive trains of 8 paced S1 beats at 8 or 10 Hz<sup>26</sup> were then followed by S2 extrastimuli every ninth beat. S1S2 intervals first equaled the pacing interval and then successively reduced by 1 msec with each nine beat cycle until ventricular refractoriness when S2 stimuli elicited no electrograms. Bipolar electrograms (BEGs) were amplified, band-pass filtered (30 Hz–1 kHz, Gould 2400S, Gould-Nicolet Technologies, Ilford, Essex, UK) and digitized (1401plus, Cambridge Electronic Design, Cambridge, UK). Computer extraction and analysis of specific electrogram features (Spike II: Cambridge Electronic Design, Cambridge,

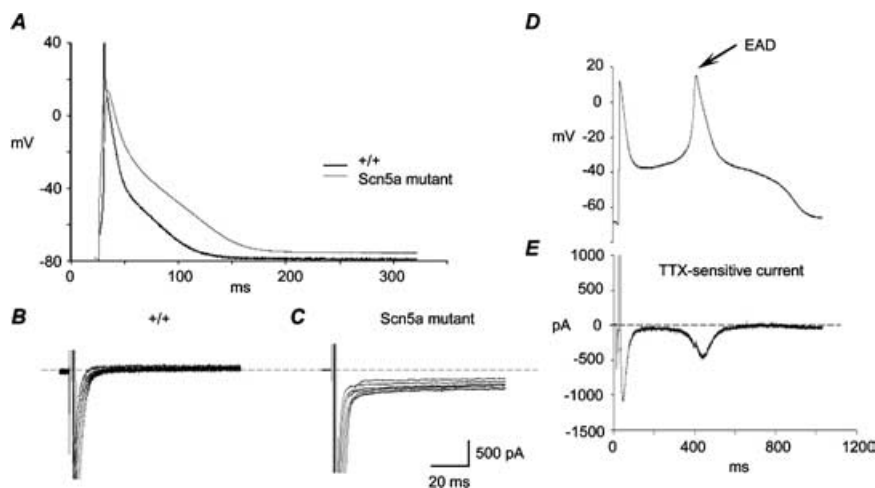


**Figure 2.** Action potential prolongation in *Scn5a* +/ $\Delta$  mutant myocytes. Microelectrode recordings from *Scn5a* +/ $\Delta$  mutant myocytes following suprathreshold stimulation showed action potentials that were prolonged relative to WT (A). In contrast to observations in WT (B), *Scn5a* +/ $\Delta$  mutant myocytes showed prolonged recovery tail currents following the termination of test pulses of duration 100 msec to a membrane potential of  $+40$  mV from a holding voltage of  $-120$  mV (C), whose current voltage relationships nevertheless closely paralleled those shown by the peak  $Na^+$  currents. *Scn5a* +/ $\Delta$  mutant myocytes also showed action potential waveforms with early afterdepolarizations (EADs) (D), which generated an inward late TTX-sensitive current when applied to myocytes in an action potential clamp (E).

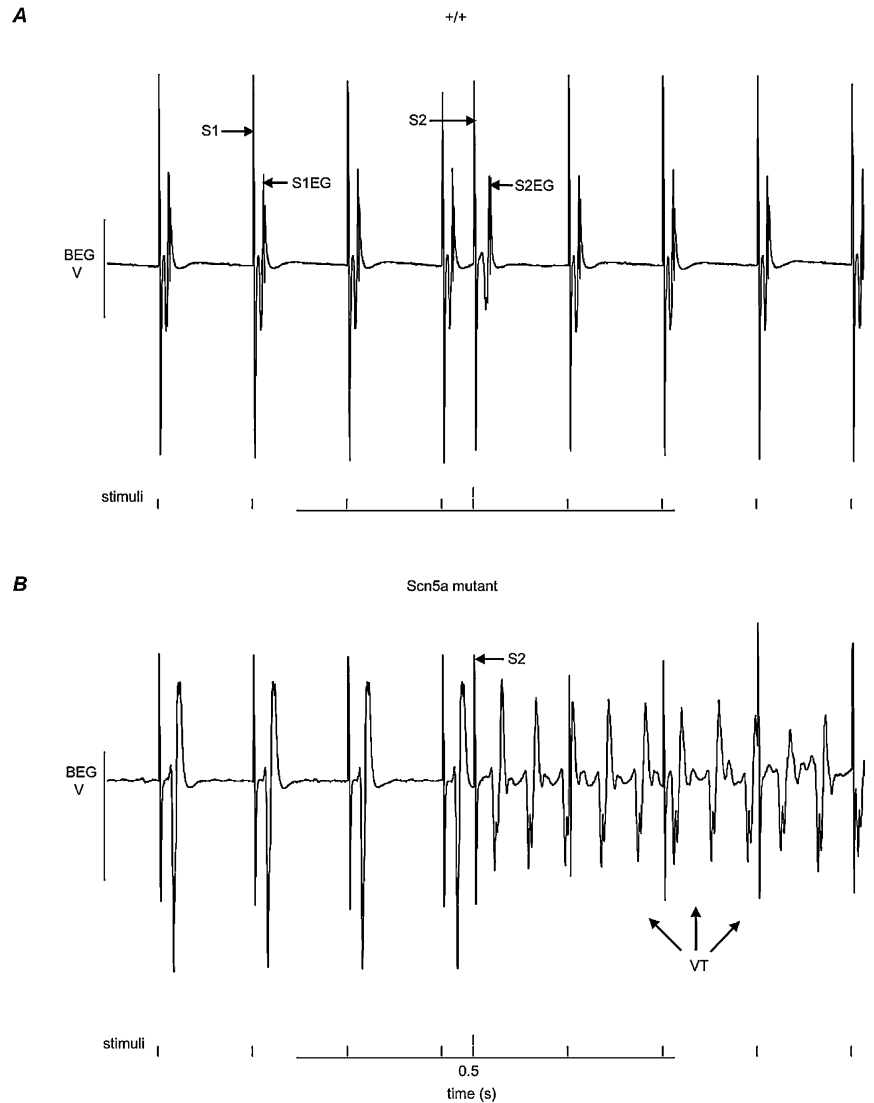


**Figure 3.** Ventricular tachycardia in *Scn5a*  $\Delta/\Delta$  mutant hearts. Representative traces from isolated perfused mouse hearts during PES. Induction of ventricular tachycardia (VT) following an S2 stimulus (delivered at a 30 msec coupling interval) in the *Scn5a*  $\Delta/\Delta$  mutant (B) but not in the WT (A) hearts at the same point in the pacing sequence. The single vertical markers at the base of each trace indicate the timings of the S1 stimuli with double vertical lines indicating the timing of S2 stimuli. BEG = bipolar electrogram; S1 = drive train stimulus; S1EG = S1 electrogram; S2 = interpolated extrastimulus; S2EG = S2 electrogram.

UK) closely paralleled clinical procedures using paced electrogram fractionation analysis (PEFA).<sup>16,17</sup> Ventricular conduction curves constructed from sequences not producing arrhythmias plotted latencies of successive electrogram peaks and troughs following S2 stimuli against corresponding S1S2 interval. The electrogram duration (EGD) was the time interval between arrivals of the first and the last electrogram peaks or troughs. Results were expressed as means  $\pm$  SEM and different experimental groups compared using ANOVA (employing SPSS software (SPSS UK Ltd., Surrey, UK)).

All drugs (Sigma-Aldrich, Poole, UK) were first prepared as 1 mM stock solutions in distilled water before dilution to the final drug concentrations in buffer. Propranolol and mexiletine stock solutions were stored at 4°C and isoproterenol stock solutions at -20°C. Hearts were perfused with drugs for 15 minutes prior to PES and PEFA studies.

## Results

Heterozygote crosses produced F2 (second) and subsequent generations: no homozygous offspring were born, suggesting embryonic lethality. Embryos were genotyped at mid-gestation (taking E 10.5 at which embryonic lethality

was observed in *Scn5a* null homozygotes as a starting point), dissected, examined, fixed, and sectioned. At E 9.5,  $+/+$ ,  $+/+$ ,  $+/+$ , and  $\Delta/\Delta$  embryos and  $+/+$  and  $\Delta/\Delta$  sections were indistinguishable. At E 10.5  $+/+$  and  $+/+$  embryos were indistinguishable but two of five  $\Delta/\Delta$  embryos were smaller than their littermates. The hearts were still beating, though irregularly in one embryo. Histological examination revealed tissue necrosis in all  $\Delta/\Delta$  embryos and none of five  $+/+$ , suggesting lethality occurring from E 10.5. Heterozygote survival was first assessed at the time of genotyping (2–6 weeks). In the presence of homozygote lethality, normal early heterozygote survival would be indicated by a 1:2 ratio of  $+/+$ : $+/+$  mice. This was not the case (Table 1). The shortfall in heterozygote numbers was not accounted for by mice found dead. The PCR used to genotype the mice was confirmed using an independent three-primer PCR, with consistent results. It is therefore possible that heterozygotes show an excess late gestational or neonatal mortality, with dead pups eaten by the mother and therefore not found. Adult mice showed no excess mortality, although following tail clipping a single  $+/+$  mouse showed a generalized seizure and died. Heterozygotes were superficially indistinguishable from WT littermates with normal weight and behavior. All heterozygotes set up for mating were fertile.

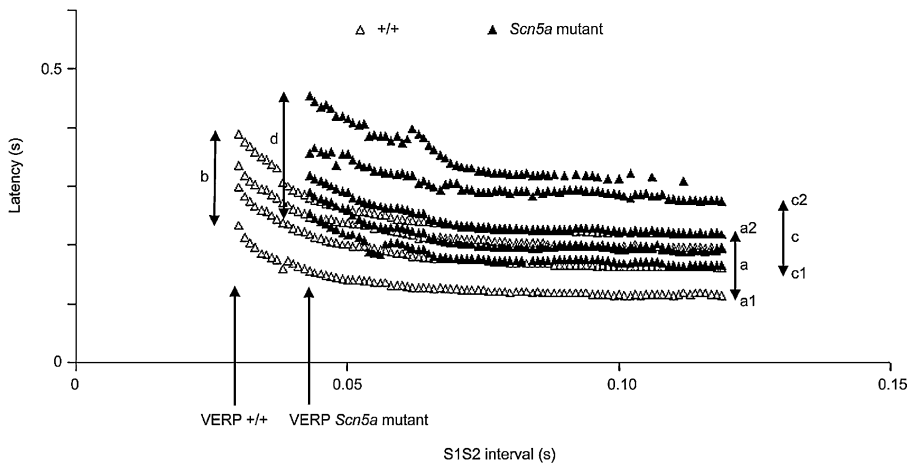


**Figure 4.** The arrhythmic tendency in *Scn5a*  $\Delta/\Delta$  mutant mouse hearts parallels a significant increase in EGD during PES. The EGD is calculated from derived conduction curves by subtracting the shortest latency (a1 or c1) from the longest latency (a2 or c2) and comparing values obtained at the beginning and end of the stimulation sequence (b/a or d/c). A significantly greater increase in EGD was seen in curves derived from *Scn5a*  $\Delta/\Delta$  mutant hearts compared to WT during PES. A greater spread in EGD is seen in the *Scn5a*  $\Delta/\Delta$  hearts as the S1S2 interval approaches the VERP for the heart when compared to WT. The VERP was also found to be significantly increased in *Scn5a*  $\Delta/\Delta$  mouse hearts when compared to WT. VERP = ventricular effective refractory period.

### Action Potential Prolongation in *Scn5a* $\Delta/\Delta$ Myocytes

Initial electrophysiological experiments confirmed recent observations<sup>18</sup> that (1) both the kinetics and steady-state distributions of activation and inactivation of the fast component of  $\text{Na}^+$  currents in patch clamp experiments (half maximal voltages ( $V_{0.5}$ ) for activation  $-56 \pm 3$  vs  $53 \pm 2.5$  mV (both  $n = 6$ ) and for inactivation  $-89 \pm 6$  vs  $-78 \pm 3$  mV (both  $n = 6$ )), (2) recovery kinetics from inactivation, did not differ between *Scn5a*  $\Delta/\Delta$  and WT myocytes, (3) current-voltage relationships of late  $\text{Na}^+$  currents resembled those of fast currents, and (4) significantly greater peak  $\text{Na}^+$  current densities occurred in *Scn5a*  $\Delta/\Delta$  ( $87.2 \pm 9.6$  pA  $\text{pF}^{-1}$ ;  $n = 7$ ) than in WT myocytes ( $36.1 \pm 4.8$  pA  $\text{pF}^{-1}$ ;  $n = 5$ ) not accounted for by differences in channel protein expression.<sup>18</sup> AP recordings from whole-cell patch electrode studies of isolated ventricular myocytes from *Scn5a*  $\Delta/\Delta$  myocytes were prolonged compared to WT ( $\text{APD}_{90} = 152 \pm 17.8$  msec ( $n = 7$ ) vs.  $55 \pm 6.6$  msec ( $n = 6$ ),  $P < 0.01$ ) (Fig. 2A). *Scn5a*  $\Delta/\Delta$  but not WT myocytes showed EADs (Fig. 2D) and persistent  $\text{Na}^+$  tail currents (Fig. 2C,B). AP clamp experiments that applied such prerecorded APs (Fig. 2D) to the same cell gave currents (Fig. 2E) showing a late inward tetrodotoxin ( $20 \mu\text{M}$ )-sensitive current coincident with the observed EAD (Fig. 2D) associated with increased risks of triggered arrhythmogenesis.

### Arrhythmic Tendency in Perfused Hearts from *Scn5a* $\Delta/\Delta$ Mice

Application of PES induced sustained ventricular tachycardias (VTs) (mean cycle length  $55 \pm 13$  msec,  $n = 8$ ) that invariably followed S2 extrastimuli delivered at S1S2 intervals close to the ventricular effective refractory interval (VERP) in 8 of 9 *Scn5a*  $\Delta/\Delta$  hearts, but consistently failed to induce VT in WT hearts ( $n = 17$ ). Figure 3 displays typical extracellular voltage traces (8 Hz drive train) from WT (top) and *Scn5a*  $\Delta/\Delta$  hearts (lower panel) at identical stages in the PES sequence: a succession of four S1 stimulus artifacts closely followed by evoked electrograms (S1EG) are succeeded by the extrastimulus artifact (S2) and its resulting electrogram (S2EG). There then follows four further S1 artifacts and electrograms in the WT heart but a sustained VT initiated by the extrastimulus in the *Scn5a*  $\Delta/\Delta$  heart. The single vertical markers beneath each trace indicate the timings of the S1 stimuli and the double vertical lines indicate the timings of the S2 stimuli.

### The Arrhythmic Tendencies in *Scn5a* $\Delta/\Delta$ Hearts Parallel Increased Electrogram Durations During PES

A recent report closely correlated positive PEFA results with increased arrhythmic risk in genetically modified mice<sup>27</sup> in parallel with previous successful risk stratifications in clinical cardiac conditions associated with arrhythmogenesis attributable to reentrant excitation.<sup>17</sup> Figure 4 shows typical conduction curves exploring for similar correlations in *Scn5a*  $\Delta/\Delta$  as opposed to WT mouse hearts undergoing PES. It plots latencies of electrogram peaks and troughs following each S2 stimulus against the corresponding S1S2 interval as this was progressively shortened to the VERP when the S2 stimulus generated no electrogram. Changes in electrogram duration (EGD) were calculated by subtracting the shortest (a1 or c1 in Fig. 4) from the longest latencies (a2 or c2) and comparing values obtained at the beginning and end of the stimulation sequence (b/a or d/c). Table 2 demonstrates that *Scn5a*  $\Delta/\Delta$  hearts showed significantly greater increases in EGD compared to WT, correlating with their greater spread in EGD, as S1S2 intervals approached VERP (Fig. 4(d) compared to (b)). They also showed greater stimulus to response latencies measured at the beginning of PES sequences (a1 and c1 in Fig. 4). Finally, *Scn5a*  $\Delta/\Delta$  mouse hearts showed

**TABLE 2**

Perfused Heart Electrophysiology

Parameter	+/+ (n)	$\Delta/\Delta$ (n)	Significance
Stimulus-response latency (msec)	$12 \pm 3$ (17)	$15 \pm 3$ (9)	$P < 0.05$
Relative increase in electrogram duration during decremental pacing (b/a in Fig. 4)	$1.25 \pm 0.17$ (17)	$1.63 \pm 0.22$ (9)	$P < 0.05$
Ventricular effective refractory period (msec)	$29 \pm 6$ (17)	$37 \pm 7$ (9)	$P < 0.05$

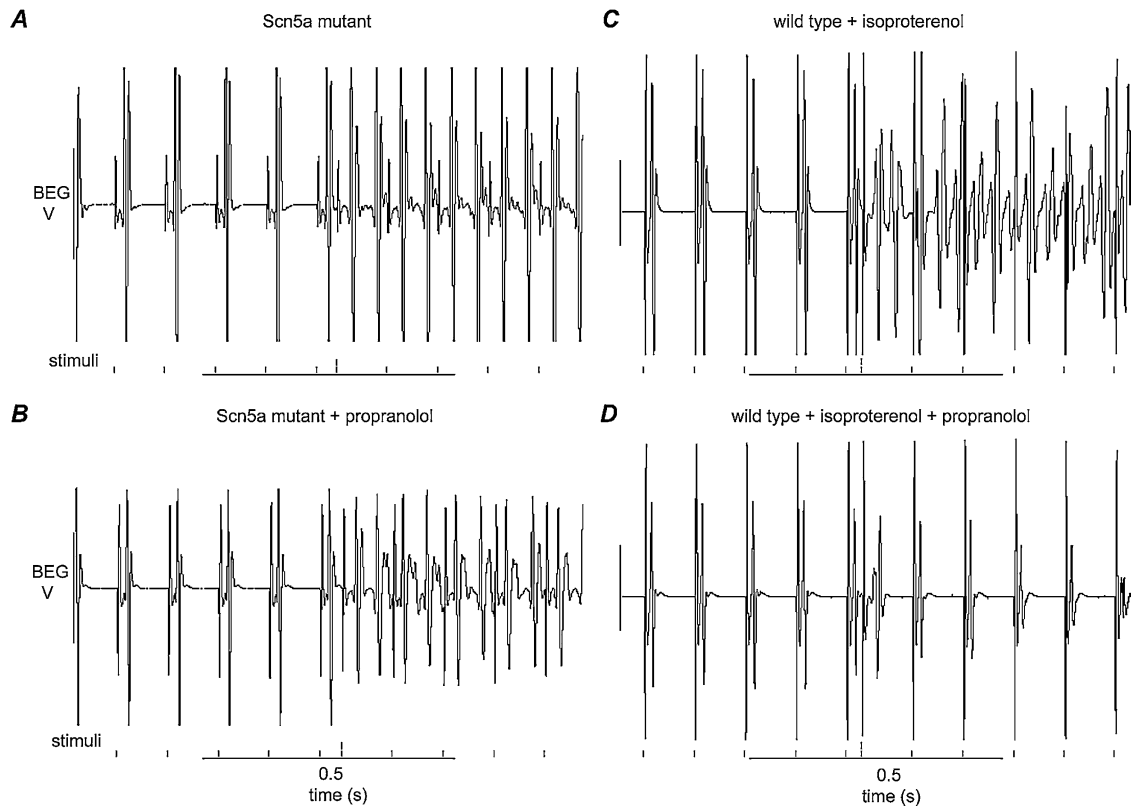


**Figure 5.** Propranolol paradoxically suppresses isoproterenol-induced arrhythmias in WT hearts but not arrhythmias in *Scn5a* +/ $\Delta$  mutant hearts. Recordings from an *Scn5a* +/ $\Delta$  mutant heart showing induction of VT in the absence (A) and following pretreatment with (B) 1  $\mu$ M propranolol. VT induction in a WT heart infused with 100 nM isoproterenol is shown (C). Following the addition of 1  $\mu$ M propranolol, the arrhythmia was suppressed in the WT heart despite the presence of 100 nM isoproterenol (D).

larger VERPs than WT ( $37 \pm 7$  msec,  $n = 9$  vs  $29 \pm 6$  msec,  $n = 17$ ,  $P < 0.05$ ; Table 2). These results thus compliment applications of PEFA to other genetically modified (*KCNE1*<sup>-/-</sup>) mouse hearts, which correlated significant increases in EGD at shortening S1S2 intervals with arrhythmic risk.<sup>27</sup>

#### **Propranolol Suppresses Isoproterenol-Induced Arrhythmias in WT Hearts but Not Arrhythmias in *Scn5a*+/ $\Delta$ Hearts**

$\beta$ -adrenergic blockers remain the preferred antiarrhythmic pharmacological agents in the management of long QT syndrome<sup>28</sup> but their efficacy in LQT3 has been questioned.<sup>13,29</sup> We assessed effects of propranolol in our arrhythmogenic, genetically modified, LQT3 model at concentrations (1  $\mu$ M) previously used successfully to study  $\beta$ -blocker effects in pharmacological LQTS models using canine left ventricular wedge preparations.<sup>12</sup> However 1  $\mu$ M propranolol conserved the arrhythmogenic phenotype in (4 of  $n = 4$ ) *Scn5a*+/ $\Delta$  mouse hearts during PES. Figure 5A,B confirms that VT occurred during PES in a *Scn5a*+/ $\Delta$  heart in the absence of propranolol but that this persisted after adding propranolol to the perfusate. Yet identical propranolol concentrations suppressed VTs during PES ( $n = 4$ ) in WT hearts previously made arrhythmogenic by infusion with 100 nM isoproterenol. Figure 5C demonstrates an induction of VT in a WT heart infused with 100 nM isoproterenol during PES, and Figure 5D, its suppression following addition of propranolol despite the continued presence of isoproterenol. Finally, comparisons of conduction curves demonstrated that 1  $\mu$ M propranolol

significantly accentuated the increases in EGD as S1S2 intervals were shortened ( $2.02 \pm 0.27$ ,  $n = 4$  vs  $1.63 \pm 0.22$ ,  $n = 9$ ,  $P < 0.05$ ) in *Scn5a*+/ $\Delta$  (Fig. 6) but not in WT hearts (Table 3).

#### **Isoproterenol Conserves Induction or Suppression of VT in *Scn5a*+/ $\Delta$ Hearts While Exerting Arrhythmic Effects in WT Hearts**

Recent reports suggested protective antiarrhythmic actions of the  $\beta$ -adrenergic agonist isoproterenol in LQT3<sup>12,18</sup> that could relate to higher frequencies of cardiac incidents in LQT3 during reduced rather than increased adrenergic activity such as rest or sleep.<sup>13</sup> We accordingly explored effects of isoproterenol concentrations (100 nM) that had previously successfully induced VT in WT mouse hearts when infused during PES in our experimental model<sup>27</sup> as shown also in Figure 5C, as well as in other pharmacological LQT3 models.<sup>12</sup> In contrast to these previous findings, isoproterenol had little effect on arrhythmogenesis in all *Scn5a*+/ $\Delta$  hearts in which PES induced VT (8 of 9 hearts studied): PES induced VT in all hearts whether before (Fig. 7A) or after (Fig. 7B) addition of isoproterenol. Furthermore, isoproterenol did not significantly alter the critical S1S2 intervals that first induced VT in *Scn5a*+/ $\Delta$  hearts (isoproterenol:  $45 \pm 5$  msec vs control:  $42 \pm 7$  msec,  $n = 8$ ). Conversely, addition of isoproterenol did not induce VT in the one *Scn5a*+/ $\Delta$  heart that did not show VT, (Fig. 7C,D) in contrast to its effects on WT hearts, during PES (Fig. 5C). Isoproterenol thus appears neither proarrhythmic nor antiarrhythmic in *Scn5a*+/ $\Delta$  hearts.

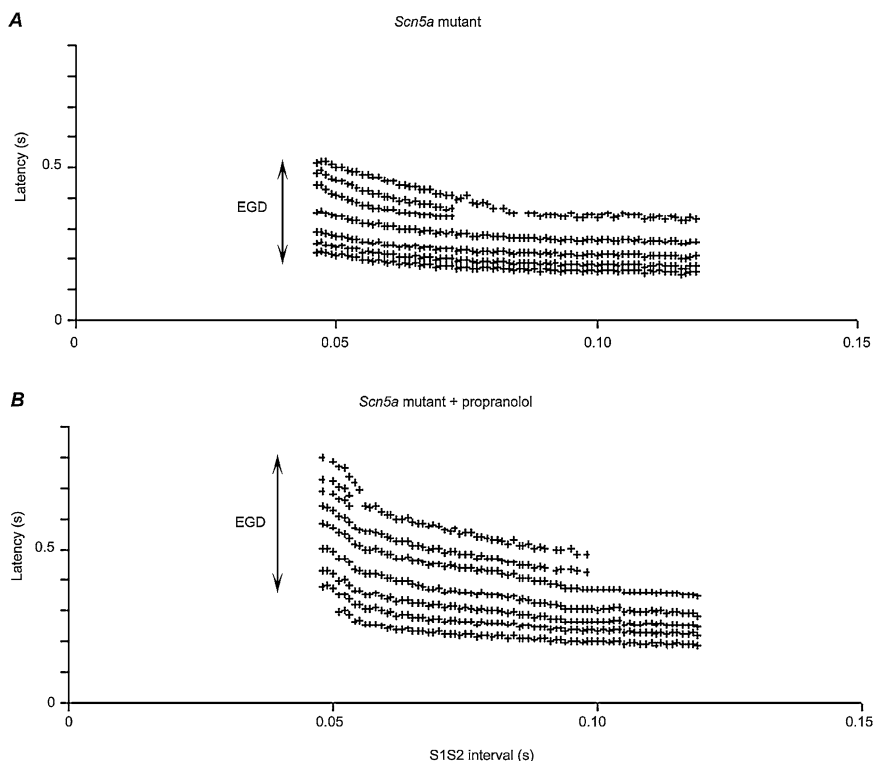


**Figure 6.** Propranolol causes a significant increase in EGD in *Scn5a* +/ $\Delta$  mutant hearts. Conduction curves derived from a *Scn5a* +/ $\Delta$  mutant heart in the absence (A) and presence (B) of 1  $\mu$ M propranolol showing a significant increase in EGD during PES when the heart was treated with 1  $\mu$ M propranolol (B).

Finally, isoproterenol did not significantly alter increases in EGD in conduction curves with shortened S1S2 intervals.

#### Mexiletine Suppresses Arrhythmias in *Scn5a*+/ $\Delta$ Hearts

The Na<sup>+</sup> channel blocker, mexiletine reduces QT intervals in human LQT3<sup>30</sup> though its role as an antiarrhythmic agent, which in such clinical situations remains contentious. In our arrhythmogenic murine model of LQT3, mexiletine concentrations (10  $\mu$ M) adopted in other pharmacological models of LQT3<sup>31,32</sup> suppressed arrhythmias in 4 of 5 *Scn5a*+/ $\Delta$  hearts. Figure 8A shows an induction of VT in a *Scn5a*+/ $\Delta$  heart during PES and Figure 8B its suppression following addition of mexiletine. However, mexiletine did not significantly alter increases in electrogram duration in conduction curves when results were analyzed using PEFA (Table 3).

#### Discussion

The present experiments explored electrophysiological features in hearts from genetically defined mice with a gain-of-function mutation associated with human LQT3 syndrome in the cardiac Na<sup>+</sup> channel gene *Scn5a*.<sup>4</sup> They assessed arrhythmic propensity in heterozygotes for the  $\Delta$ KPQ mutation (*Scn5a*+/ $\Delta$ ) by using PES and a modification of PEFA,

which has previously been used to quantify an arrhythmic substrate using conduction delay in human hypertrophic cardiomyopathy.<sup>17,33</sup> More recent studies have demonstrated its applicability to transgenic mouse LQT5 models.<sup>27</sup> We observed parallels with myocytes from *Scn5a*+/ $\Delta$  mice already produced by Nuyens<sup>18</sup> including homozygote lethality, prolonged APs, late Na<sup>+</sup> current following voltage steps, EADs during late Na<sup>+</sup> current phases, and elevated peak Na<sup>+</sup> current densities. Both mutant *Scn5a*+/ $\Delta$  Na<sup>+</sup> channels showed similar steady state current voltage, conductance voltage, activation and inactivation curves, recoveries from inactivation, and long current tails following long depolarizing steps to  $-10$  mV.

Applications of both PES and PEFA in whole perfused hearts to our *Scn5a*+/ $\Delta$  system demonstrated for the first time similarities and contrasts with both the corresponding human LQT3 syndrome and two other physiological, guinea pig myocyte and perfused canine left ventricle wedge, preparations. First, most LQT3 patients are heterozygous for the  $\Delta$ KPQ *Scn5a* mutation suggesting homozygote lethality. There is only one reported homozygous pediatric case that presented with syncope, QTc prolongation, and atrioventricular block. Whole-cell patch clamp analysis of the mutant human channel using transfected human embryonic kidney HEK 293 cells then revealed the typical persistent inward Na<sup>+</sup> current of LQT3.<sup>34</sup> In common with the earlier *Scn5a*+/ $\Delta$  system,<sup>18</sup> we observed only heterozygote neonatal mice. Our further gestational genotyping studies suggested embryonic homozygote lethality. At E 9.5, WT, +/ $\Delta$ , and  $\Delta$ / $\Delta$  embryos were macroscopically indistinguishable. At E 10.5, WT and +/ $\Delta$  remained indistinguishable, but necrosis of the  $\Delta$ / $\Delta$  offspring had begun. No mutant embryos survived to term.

Secondly, LQTS is strongly associated with prolonged ventricular repolarization<sup>13,35-37</sup> and tendency to ventricular

**TABLE 3**

Effect of Pharmacological Agents on *Scn5a* +/ $\Delta$  Mouse Hearts

Drug	Arrhythmia Suppression	Effect on Increase in EGD
Propranolol	No (0 of 4)	Greater increase
Mexiletine	Yes (4 of 4)	No significant difference
Isoproterenol	No (0 of 6)	No significant difference

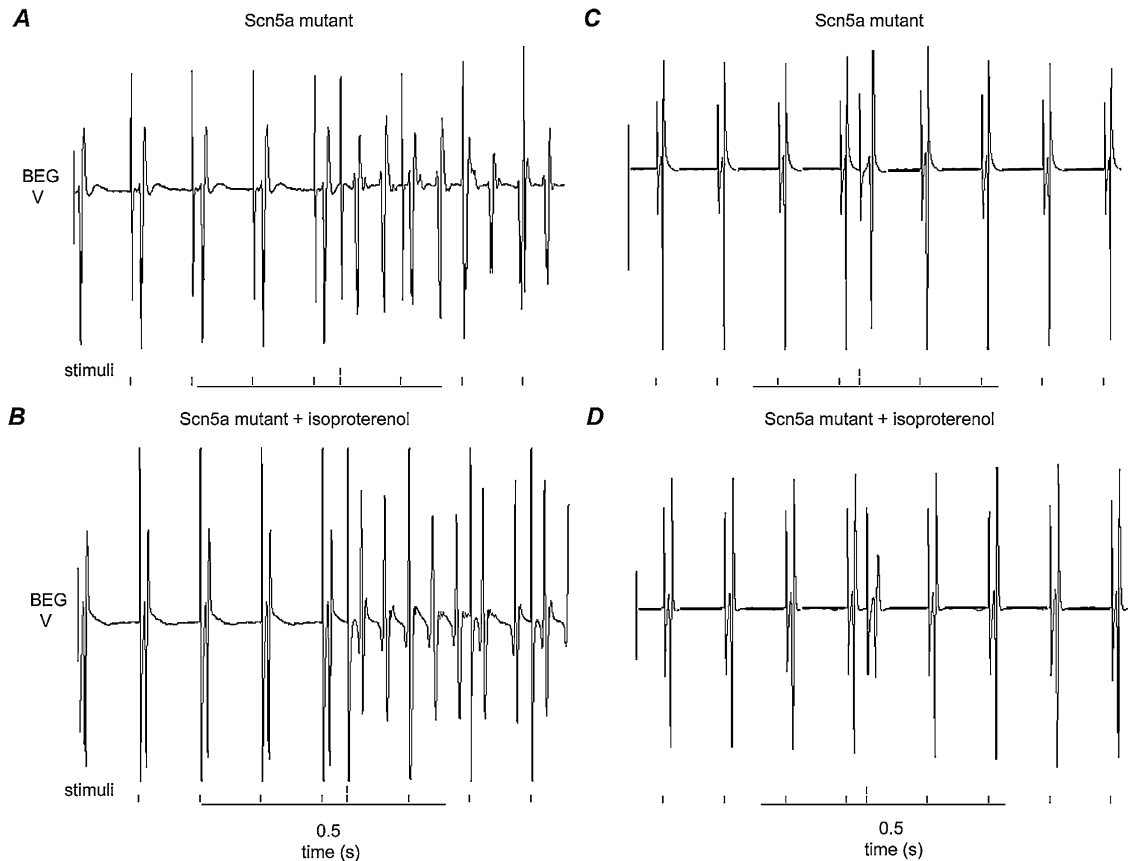


**Figure 7.** Isoproterenol has little effect on arrhythmia induction or suppression in *Scn5a*  $+/\Delta$  mutant hearts in contrast to its arrhythmic effects in WT hearts. Induction of VT in a *Scn5a*  $+/\Delta$  mutant heart in the absence (A) and presence (B) of 100 nM isoproterenol. In the 1 *Scn5a*  $+/\Delta$  heart that was studied in which VT was not seen during PES, shown in (C), addition of isoproterenol did not result in the induction of VT (D).

arrhythmia, particularly TdP, leading to syncope and sudden cardiac death.<sup>38</sup> We report that critically timed S2 extrastimuli that mimic EAD activity, similarly induced VT in *Scn5a*  $+/\Delta$  hearts but not WT controls.

Thirdly, quantitative analysis of electrical conduction, adapting PEFA, yielded significant differences in critical values that suggested arrhythmogenic tendency in *Scn5a*  $+/\Delta$ . PEFA is established for the stratification of patients with conditions including hypertrophic cardiomyopathy, idiopathic ventricular fibrillation, and LQTS, that increase risk of ventricular arrhythmia through reentrant excitation.<sup>17</sup> Current opinion suggests that TdP in human LQT3 is initiated by a triggered mechanism, then maintained by reentrant excitation.<sup>39–41</sup> Similarly, increased reentrant tendencies appear to correlate with the increased spatial dispersion of repolarization seen in other animal models such as anthopleura toxin A (AP-A) treated guinea pig myocytes and canine wedge preparations exposed to anemone toxin (ATX-II).<sup>12,40</sup> The present study on *Scn5a*  $+/\Delta$  mice showed increased EGDs and dispersed conduction curves that displayed a greater spread of values as SIS2 intervals approached VERP. Such inhomogeneous repolarization and propensity to arrhythmia has been reported previously in other LQTS transgenic mice.<sup>27</sup>

Fourthly, adrenergic stimulation through exercise, stress, or startle triggers arrhythmia in most LQTS subtypes, particularly LQT1 and LQT2.<sup>13</sup> Catecholamine-induced arrhythmia also occurs in LQT3 but a significant proportion of

arrhythmic events occur during rest or sleep.<sup>18</sup> Furthermore, increased heart rate appears to produce an exaggerated shortening of the QT interval in patients with LQT3.<sup>42</sup> In guinea pig ventricular myocytes,  $\beta$ -adrenergic stimulation with isoproterenol had minimal effects on APD. However, the same stimulation applied to myocytes treated with anthopleura toxin A that inhibits  $\text{Na}^+$  current inactivation, significantly reduces APD.<sup>31</sup> Another animal model applies anemone toxin (ATX-II) to augment late  $I_{\text{Na}}$  in arterially perfused wedge preparations of canine left ventricle; isoproterenol treatment then consistently abbreviated  $\text{APD}_{90}$  and suppressed TdP, effects reversed by propranolol. Nuyens similarly reported that isoproterenol protected 3 of 4  $\Delta$ KPQ *Scn5a*  $+/\Delta$  mice against VT and reduced arrhythmia duration in the fourth.<sup>18</sup> However, in the present study the same dose of isoproterenol (100 nM) did not protect *Scn5a*  $+/\Delta$  hearts against VT.

Fifthly, LQTS is generically treated by  $\beta$ -adrenoreceptor blockade,<sup>28</sup> yet its clear benefits in LQT1 and LQT2 are not seen in LQT3 patients.<sup>29,43</sup> Nevertheless, despite the antiarrhythmic effects of  $\beta$ -adrenergic stimulation<sup>18</sup>  $\beta$ -blockade might remain beneficial by suppressing arrhythmogenic sudden rate accelerations or premature beats that occur during sympathetic surges.<sup>18</sup> However, we report that propranolol (1  $\mu\text{M}$ ) failed to protect against VT in *Scn5a*  $+/\Delta$  mutants ( $n = 4$ ) yet prevented arrhythmia in all WT controls ( $n = 4$ ). Indeed, it significantly increased EGD and dispersion in conduction curves specifically in *Scn5a*  $+/\Delta$  hearts during PES. Thus  $\beta$ -blockade could actually accentuate the

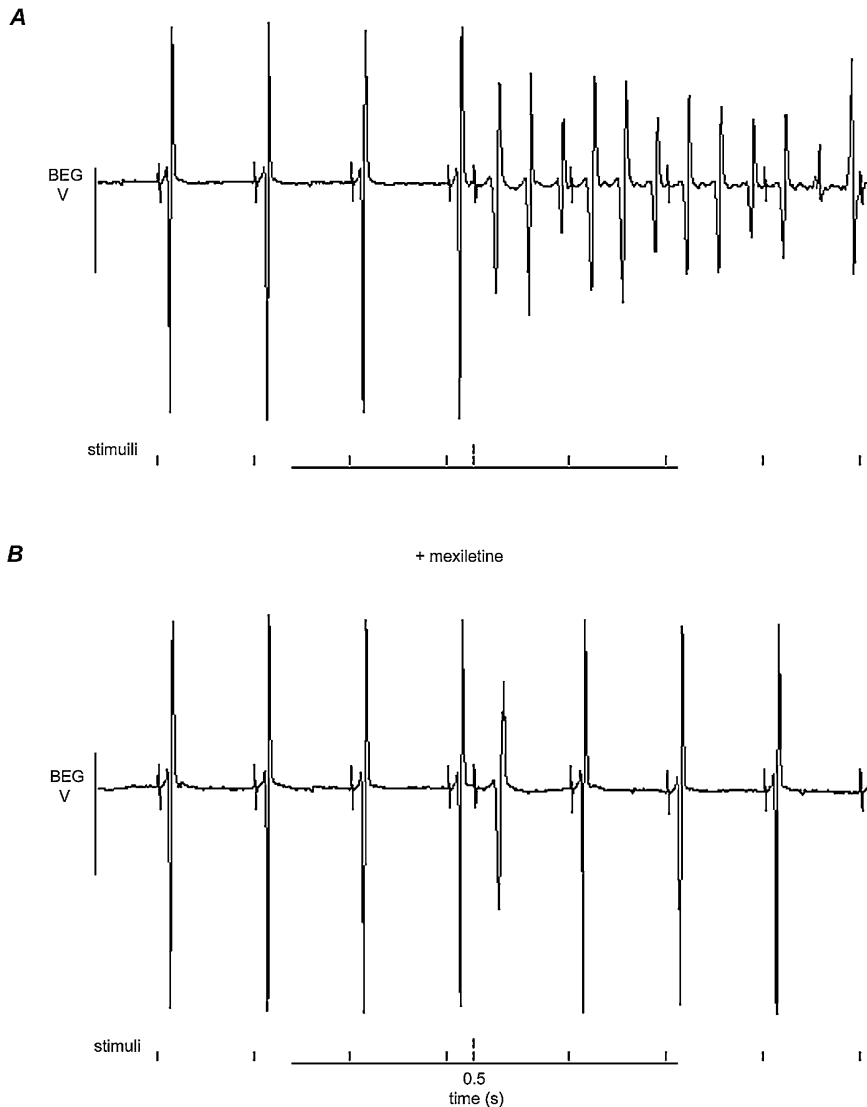


**Figure 8.** Mexiletine suppresses arrhythmias in *Scn5a* +/Δ mutant hearts. Induction of VT in a *Scn5a* +/Δ mutant mouse heart during PES (A). Following addition of 10 μM mexiletine, no arrhythmia induction is seen during PES (B). Both traces are at the same point in the pacing sequence.

preexisting reentrant substrate in LQT3. This may be due to enhanced heterogeneity of repolarization, exaggerated action potential prolongation, or facilitation of pause-dependent TdP.

Finally, the class 1b antiarrhythmic drug mexiletine is known to reduce QT intervals in LQT3 patients.<sup>42</sup> In other LQT3 animal models, mexiletine reduces APD in anthopleurotoxin A (AP-A)-treated guinea pig ventricular myocytes<sup>31</sup> and reduces transmural dispersion of repolarization in canine wedge preparations exposed to anemone toxin (ATX-II).<sup>44</sup> It shortens APD and suppresses EADs in mice with a heterozygous knock-in ΔKPQ *Scn5a*+/Δ deletion (*Scn5a*-Tg), particularly at long cycle lengths.<sup>45</sup> The present experiments demonstrated similar antiarrhythmic effects in 4 of 5 *Scn5a*+/Δ mice, but no changes in conduction curves using PEFA. The latter observation might reflect mexiletine exerting its antiarrhythmic effects through suppression of triggered rather than reentrant arrhythmias (cf<sup>27</sup>). If so, the present findings suggest at least two arrhythmic mechanisms in LQT3. First, a reentrant mechanism, enhanced by β-adrenoreceptor blockade is suggested by the neutral effect of propranolol on *Scn5a*+/Δ but antiarrhythmic effect on WT hearts, and the in-

creased dispersal of *Scn5a*+/Δ conduction curves. Secondly, a triggered mechanism suppressed by mexiletine, suggested by its antiarrhythmic effect with no change in conduction curves, might initiate arrhythmia. Such speculation merits further investigation.

*Acknowledgments:* We would like to thank Rosemary Thresher and Sandra Webb for skilled assistance.

## References

1. Lehmann-Horn F, Jurkat-Rott K: Voltage-gated ion channels and hereditary disease: *Physiol Rev* 1999;79:1317-1372.
2. Schwartz PJ, Priori SG, Napolitano C: The long QT syndrome. In Zipes DP, Jalife J, eds: *Cardiac Electrophysiology: From Cell to Bedside*. Philadelphia, PA: WB Saunders Co, 2000, pp. 597-615.
3. Clancy CE, Kass RS: Inherited and acquired vulnerability to ventricular arrhythmias: Cardiac Na<sup>+</sup> and K<sup>+</sup> channels. *Physiol Rev* 2005;85:33-47.
4. Wang Q, Shen J, Li Z, Timothy K, Vincent GM, Priori SG, Schwartz PJ, Keating MT: Cardiac sodium channel mutations in patients with long QT syndrome, an inherited cardiac arrhythmia. *Hum Mol Genet* 1995;4:1603-1607.

5. Wang Q, Shen J, Splawski I, Atkinson D, Li Z, Robinson JL, Moss AJ, Towbin JA, Keating MT: SCN5A mutations associated with an inherited cardiac arrhythmia, long QT syndrome. *Cell* 1995;80:805-811.
6. Wattanasirichaigoon D, Vesely MR, Duggal P, Levine JC, Blume ED, Wolff GS, Edwards SB, Beggs AH: Sodium channel abnormalities are infrequent in patients with long QT syndrome: Identification of two novel SCN5A mutations. *Am J Med Genet* 1999;86:470-476.
7. Splawski I, Shen J, Timothy KW, Lehmann MH, Priori S, Robinson JL, Moss AJ, Schwartz PJ, Towbin JA, Vincent GM, Keating MT: Spectrum of mutations in long-QT syndrome genes. KVLQT1, HERG, SCN5A, KCNE1, and KCNE2. *Circulation* 2000;102:1178-1185.
8. January CT, Riddle JM: Early afterdepolarizations: Mechanism of induction and block. A role for L-type Ca<sup>2+</sup> current. *Circ Res* 1989;64:977-990.
9. Tan HL, Hou CJ, Lauer MR, Sung RJ: Electrophysiologic mechanisms of the long QT interval syndromes and torsade de pointes. *Ann Intern Med* 1995;122:701-714.
10. Antzelevitch C, Shimizu W: Cellular mechanisms underlying the long QT syndrome. *Curr Opin Cardiol* 2002;17:43-51.
11. El-Sherif N, Chinushi M, Caref EB, Restivo M: Electrophysiological mechanism of the characteristic electrocardiographic morphology of torsade de pointes tachyarrhythmias in the long-QT syndrome: Detailed analysis of ventricular tridimensional activation patterns. *Circulation* 1997;96:4392-4399.
12. Shimizu W, Antzelevitch C: Differential effects of beta-adrenergic agonists and antagonists in LQT1, LQT2 and LQT3 models of the long QT syndrome. *J Am Coll Cardiol* 2000;35:778-786.
13. Schwartz PJ, Priori SG, Spazzolini C, Moss AJ, Vincent GM, Napolitano C, Denjoy I, Guicheney P, Breithardt G, Keating MT, Towbin JA, Beggs AH, Brink P, Wilde AA, Toivonen L, Zareba W, Robinson JL, Timothy KW, Corfield V, Wattanasirichaigoon D, Corbett C, Haverkamp W, Schulze-Bahr E, Lehmann MH, Schwartz K, Coumel P, Bloise R: Genotype-phenotype correlation in the long-QT syndrome: Gene-specific triggers for life-threatening arrhythmias. *Circulation* 2001;103:89-95.
14. Zareba W, Sattari MN, Rosero S, Couderc JP, Moss AJ: Altered atrial, atrioventricular, and ventricular conduction in patients with the long QT syndrome caused by the DeltaKPQ SCN5A sodium channel gene mutation. *Am J Cardiol* 2001;88:1311-1314.
15. van den Berg MP, Wilde AA, Viersma TJW, Brouwer J, Haaksma J, van der Hout AH, Stolte-Dijkstra I, Bezzina TCR, Van Langen IM, Beaufort-Krol GC, Cornel JH 2nd, Crijns HJ: Possible bradycardic mode of death and successful pacemaker treatment in a large family with features of long QT syndrome type 3 and Brugada syndrome. *J Cardiovasc Electrophysiol* 2001;12:630-636.
16. Saumarez RC, Grace AA: Paced ventricular electrogram fractionation and sudden death in hypertrophic cardiomyopathy and other non-coronary heart diseases. *Cardiovasc Res* 2000;47:11-22.
17. Saumarez RC, Chojnowska L, Derksen R, Pytkowski M, Sterlinski M, Huang CL, Sadoul N, Hauer RN, Ruzyllo W, Grace AA: Sudden death in noncoronary heart disease is associated with delayed paced ventricular activation. *Circulation* 2003;107:2595-2600.
18. Nuyens D, Stengl M, Dugarmaa S, Rossenbacker T, Compennolle V, Rudy Y, Smits JF, Flameng W, Clancy CE, Moons L, Vos MA, Dewerchin M, Benndorf K, Collen D, Carmeliet E, Carmeliet P: Abrupt rate accelerations or premature beats cause life-threatening arrhythmias in mice with long-QT3 syndrome. *Nat Med* 2001;7:1021-1027.
19. Yagi T, Nada S, Watanabe N, Tamemoto H, Kohmura N, Ikawa Y, Aizawa S: A novel negative selection for homologous recombinants using diphtheria toxin A fragment gene. *Anal Biochem* 1993;214:77-86.
20. Bradley A, Evans M, Kaufman MH, Robertson E: Formation of germline chimaeras from embryo-derived teratocarcinoma cell lines. *Nature* 1984;309:255-256.
21. Braun RE, Lo D, Pinkert CA, Wiedera G, Flavell RA, Palmiter RD, Brinster RL: Infertility in male transgenic mice: Disruption of sperm development by HSV-tk expression in postmeiotic germ cells. *Biol Reprod* 1990;43:684-693.
22. al-Shawi R, Burke J, Wallace H, Jones C, Harrison S, Buxton D, Maley S, Chandley A, Bishop JO: The herpes simplex virus type 1 thymidine kinase is expressed in the testes of transgenic mice under the control of a cryptic promoter. *Mol Cell Biol* 1991;11:4207-4216.
23. Ashley EA, Sears CE, Bryant SM, Watkins HC, Casadei B: Cardiac nitric oxide synthase 1 regulates basal and  $\beta$ -adrenergic contractility in murine ventricular myocytes. *Circulation* 2002;105:3011-3016.
24. Linz KW, Meyer R: Control of L-type calcium current during the action potential of guinea-pig ventricular myocytes. *J Physiol* 1998;513:425-442.
25. Langendorff O: Untersuchungen am überlebenden Säugetierherzen. *Pflügers Arch Gesamte Physiol* 1895;61:291-332.
26. Papadatos GA, Wallerstein PM, Head CE, Head CE, Ratcliff R, Brady PA, Benndorf K, Saumarez RC, Trezise AE, Huang CL, Vandenberg JI, Colledge WH, Grace AA: From the Cover: Slowed conduction and ventricular tachycardia after targeted disruption of the cardiac sodium channel gene *Scn5a*. *Proc Natl Acad Sci USA* 2002;99: 6210-6215.
27. Balasubramaniam R, Grace AA, Saumarez RC, Vandenberg JI, Huang CL: Electrogram prolongation and nifedipine-suppressible ventricular arrhythmias in mice following targeted disruption of KCNE1. *J Physiol* 2003;552:535-546.
28. Moss AJ: Management of patients with the hereditary long QT syndrome. *J Cardiovasc Electrophysiol* 1998;9:668-674.
29. Priori SG, Napolitano C, Schwartz PJ, Grillo M, Bloise R, Ronchetti E, Moncalvo C, Tulipani C, Veia A, Bottelli G, Nastoli J: Association of long QT syndrome loci and cardiac events among patients treated with beta-blockers. *JAMA* 2004;292:1341-1344.
30. Schwartz PJ, Priori SG, Locati EH, Napolitano C, Cantu F, Towbin JA, Keating MT, Hammoude H, Brown AM, Chen LS: Long QT syndrome patients with mutations of the SCN5A and HERG genes have differential responses to Na<sup>+</sup> channel blockade and to increases in heart rate. Implications for gene-specific therapy. *Circulation* 1995;92:3381-3386.
31. Priori SG, Napolitano C, Cantu F, Brown AM, Schwartz PJ: Differential response to Na<sup>+</sup> channel blockade,  $\beta$ -adrenergic stimulation, and rapid pacing in a cellular model mimicking the SCN5A and HERG defects present in the long-QT syndrome. *Circ Res* 1996;78:1009-1015.
32. Shimizu W, Antzelevitch C: Sodium channel block with mexiletine is effective in reducing dispersion of repolarization and preventing torsade des pointes in LQT2 and LQT3 models of the long-QT syndrome. *Circulation* 1997;96:2038-2047.
33. Saumarez RC, Slade AK, Grace AA, Sadoul N, Camm AJ, McKenna WJ: The significance of paced electrogram fractionation in hypertrophic cardiomyopathy. A prospective study. *Circulation* 1995;91:2762-2768.
34. Lupoglazoff JM, Cheav T, Baroudi G, Berthet M, Denjoy I, Cauchemez B, Extramiana F, Chahine M, Guicheney P: Homozygous SCN5A mutation in long-QT syndrome with functional two-to-one atrioventricular block. *Circ Res* 2001;89:E16-21.
35. Bennett PB, Yazawa K, Makita N, George AL Jr: Molecular mechanism for an inherited cardiac arrhythmia. *Nature* 1995;376:683-685.
36. Dumaine R, Wang Q, Keating MT, Hartmann HA, Schwartz PJ, Brown AM, Kirsch GE: Multiple mechanisms of Na<sup>+</sup> channel—Linked long-QT syndrome. *Circ Res* 1996;78:916-924.
37. Wang DW, Yazawa K, George AL Jr, Bennett PB: Characterization of human cardiac Na<sup>+</sup> channel mutations in the congenital long QT syndrome. *Proc Natl Acad Sci USA* 1996;93:13200-13205.
38. Moss AJ, Schwartz PJ, Crampton RS, Zivoni D, Locati EH, MacCluer J, Hall WJ, Weikamp L, Vincent GM, Garson A Jr: The long QT syndrome. Prospective longitudinal study of 328 families. *Circulation* 1991;84:1136-1144.
39. El-Sherif N: Mechanism of ventricular arrhythmias in the long QT syndrome: On hermeneutics. *J Cardiovasc Electrophysiol* 2001;12:973-976.
40. Restivo M, Caref EB, Kozhevnikov DO, El-Sherif N: Spatial dispersion of repolarization is a key factor in the arrhythmogenicity of long QT syndrome. *J Cardiovasc Electrophysiol* 2004;15:323-331.
41. Yan GX, Wu Y, Liu T, Wang J, Marinchak RA, Kowey PR: Phase 2 early afterdepolarization as a trigger of polymorphic ventricular tachycardia in acquired long-QT syndrome: Direct evidence from intracellular recordings in the intact left ventricular wall. *Circulation* 2001;103:2851-2856.
42. Schwartz PJ, Priori SG, Locati EH, Napolitano C, Cantu F, Towbin JA, Keating MT, Hammoude H, Brown AM, Chen L-SK, Colatsky TJ: Long QT syndrome patients with mutations of the SCN5A and HERG genes have differential responses to Na<sup>+</sup> channel blockade and to increases in heart rate: Implications for gene-specific therapy. *Circulation* 1995;92:3381-3386.

43. Moss AJ, Zareba W, Hall WJ, Schwartz PJ, Crampton RS, Benhorin J, Vincent GM, Locati EH, Priori SG, Napolitano C, Medina A, Zhang L, Robinson JL, Timothy K, Towbin JA, Andrews ML: Effectiveness and limitations of beta-blocker therapy in congenital long-QT syndrome. *Circulation* 2000;101:616-623.
44. Shimizu W, Antzelevitch C: Sodium channel block with mexiletine is effective in reducing dispersion of repolarization and preventing torsade de pointes in LQT2 and LQT3 models of the long-QT syndrome. *Circulation* 1997;96:2038-2047.
45. Fabritz L, Kirchhof P, Franz MR, Nuyens D, Rossenbacker T, Ottenhof A, Haverkamp W, Breithardt G, Carmeliet E, Carmeliet P: Effect of pacing and mexiletine on dispersion of repolarisation and arrhythmias in  $\Delta$ KPQ SCN5A (long QT3) mice. *Cardiovasc Res* 2003;57:1085-1093.